SSRG International Journal of Electronics and Communication Engineering
ISSN: 2348-8549/ https://doi.org/10.14445/23488549/IJECE-V13I2P109

Volume 13 Issue 2, 115-132, February 2026

Original Article

6G Edge-Networks Integrated Intelligent Graph-based Learning Model for Heterogeneous Clustered Hybrid UAV in Wireless Powered IoT Communication

G. Ramkumar

Department of Electronics and Communication Engineering, Saveetha School of Engineering, Saveetha Institute of Medical and Technical Sciences (SIMATS), Chennai, India.

Corresponding Author : pgrvlsi@gmail.com

Received: 18 November 2025 Revised: 20 December 2025 Accepted: 21 January 2026 Published: 20 February 2026

Abstract *- The Hybrid Unmanned Aerial Vehicles (UAVs) are getting significant ground in their role as a source of information exchange. This article presents a new network architecture of hybrid UAVs incorporating edge-based federated learning, spectrum sensing, and graph-based learning models referred to as Intelligent Learning of Heterogeneous Clustered Hybrid UAV (ILHCHU) to enhance information sharing and throughput. The proposed system will use UAVs as the supplementary computing platforms and communication stations, which will provide an aerial view of the environment and help to detect possible road hazards. The architecture includes a K-means Clustering Algorithm to enhance resource distribution and a probabilistic model-checking to improve battery efficiency. An Intelligent Graph Learning Model (IGLM) is used to collect observation data from adjacent agents, targets, and obstacles. The throughput of the system is evaluated using a saturation throughput model, accounting for packet loss, opportunity loss, and missed detections. Simulation demonstration illustrates that ILHCHU improves information sharing and throughput within a 6G edge network. The results of the simulation are carried out with the following parameter matrices: communication steps, unassigned tasks, total score, running time, time consumed, energy consumption, coverage, repeated rate, and communication composition. Utilizing this metric, the ILHCHU model is compared with the earlier baseline methodologies, and achieved the least number of communication steps at 70000, 20 unassigned tasks, a lower total score of 12000, a running time of 80, a time consumed of 185, a greater energy consumption figure of 750, and a coverage rate and repeated coverage rate of 97 and 33, respectively, as well as communication steps of 5000 and a communication composition of 8 all accomplished by our proposed ILHCHU model. The hybrid UAV-assisted communication system displays the potential to improve connectivity, optimize resource usage, and monitor the system environment, positioning it as a key solution for 6G edge networks in wireless powered IoT applications.*

Keywords *- Unmanned Aerial Vehicle (UAV), Intelligent Graph Learning Model (IGLM), 6G Edge Network, K-means Clustering Algorithm, Wireless Powered IoT.*

1. Introduction

Due to their remarkable adaptability and reliable self-organization, UAVs have become widely used across many areas. Multi-UAVs have attracted more attention than individual model because of their capability to accomplish demanding and intricate tasks effectively and efficiently in both civilian and military sectors [1]. They are also more resistant to failures. Multi-UAV implementation enhances efficiency in the system because it allows the simultaneous execution of tasks. Simply put, a framework is used to enable different models of UAVs to cooperate and share duties, thereby increasing the level of autonomy of the system. Nonetheless, despite the intensive study of UAV task allocation, it is still possible to improve it. With the increased number of UAVs, frequent communication is imperative to share duties among the UAVs, and this requires a lot of computing and reliable communication with the allocation of resources. Equally, multiple UAVs establish direct communication between them to facilitate information sharing to make a reliable and efficient network essential in distributing tasks. Edge networks use UAVs and MEC to enhance the processing of data near the origin to reduce latency and bandwidth needs [2]. UAVs perform the role of mobile base stations or relays that are necessary during times of disaster when the terrestrial infrastructure is destroyed. Optimization strategies such as fuzzy logic and reinforcement learning improve resource allocation, energy use, and task delegation to edge servers or LEO satellites. Advanced architectures ensure scalability and reliable communication, supporting IoT devices in changing environments.

UAV-IoT networks focus on increasing energy efficiency, improving communication, and managing resources [3]. The Energy Optimization Framework is

designed to work with UAV-IoT networks by combining energy-gathering models and effective resource-allocation methodologies. It ensures that UAVs and IoT devices will remain within power constraints so that they can work longer hours without sacrificing communication efficiency. Signal quality can be improved by modelling SINR, which leads to a better quality of communication [4]. The model is helpful in accounting for self-interference, environmental noise, and inter-cell interference, which have given a more reliable performance measurement of full-duplex operations within UAV-IoT systems. The application of the Lagrangian Multiplier Method in optimizing the allocation of resources is a sophisticated method used in UAV-IoT networks. This will be a good compromise between power limitations, energy savings, and communication capability, to serve the interests of interference management and network stability [5].

The integration of UAVs into edge networks of 6G demonstrates that they can provide reliable communication services to problematic sites. Uncrewed aerial vehicles raise awareness of different scenarios, such as the identification of hazards, search and rescue operations, and environmental surveillance. Better Techniques of Clustering to achieve a Good Communication also involve a better k-means++ clustering algorithm, which increases the cluster formation in UAV-IoT networks. It will increase the cooperation among UAVs and IoT devices, as well as the effectiveness of data transmission, and reduce energy consumption across the network. The Data Aggregation objective, with the help of IGLM, is to enhance the process of collecting data covering the geographically distributed UAVs and IoT devices. IGLM enables the network to adapt to the changing conditions in a smooth manner, which increases decision-making and improves the overall performance of UAV-IoT communication systems. In the UAV-IoT, Federated Learning supports privacy-preserving and secure collaboration, which enhances decentralized decision-making. This approach will ensure that privacy is upheld and inter-device learning can be achieved, which eventually enhances the flexibility and robustness of the system to real-time use.

2. Related Work

In [6], the author discusses the use of IoT technology in environmental monitoring, where sensor nodes transmit information to a wireless gateway or UAV. The Deep UAV algorithm maximizes the effectiveness of data collection and energy consumption. The author is talking about difficulties in the optimization of UAV data collection in complicated environments in [7]. Through Deep Learning, the increase in energy efficiency and data collection may be significant. In [8], the application of UAVs in Federated Learning enhances the energy efficiency of devices using alternate optimization algorithms of optimized flight paths. In [9], the author discusses the use of quadrotor UAVs in the IoT networks with the aim of energy optimization. They present a UAV energy consumption model. A Quadrotor UAV has been used in [10] to optimize the IoT networks, as it collects data effectively, and the FCC trajectory has been presented to minimize the consumption of energy. In [11], the article discusses the application of UAV-mounted relays in order to increase the coverage and reliability of IoT systems. NOMA and device grouping are effective in data transmission optimization, and antenna selection improves their performance. In [12], an EEUCH protocol improves the collection of data in remote WSNs to IoT through sensors with WuRs triggered by UAV signals, thereby making it more efficient. In [13], the author considers communication delay in the formation control in UAV surveillance systems and suggests DIMDP and DIDDPG algorithms. At [14], UAVs are used to expand the wireless coverage, and energy efficiency and tradeoffs are analysed in a game context through the deployment of small cells. The author in [15] proposes the use of MEC servers in enhancing the capacity of power facilities to be inspected by the UAVs with the aim of increasing energy efficiency and processing of tasks. The author in the article [16] suggests the application of DE and GBO algorithms to optimize UAV deployment in IoT applications, which will lead to an increase in efficiency and convergence. The author, in [17], examines problems in access and communication in IoT and suggests a cross-layer computing architecture, which incorporates the use of Deep Learning. In [18], 5G, renewable energy sources, and minimizing hops are used to extend an IoUT communication, as well as reduce interference and research issues. In [19], the author investigates UAVs and Mobile Edge Computing in the disaster zones and suggests a novel optimization algorithm to ensure efficiency. The author offers a decision-making scheme of 6G networks in [20], using UAV migration to address traffic bursts and coverage of the services.

In [21], a blockchain of IoT with UAVs is used to provide security and efficiency. They perform the role of edge nodes and receive charging coins for data forwarding. A predictive algorithm is adaptive and uses less energy. With the use of BaaS, MEC, cloud servers, peer devices, and UAVs, the author examines the pricing and resource management of IoT in [22]. Endorses reinforcement learning. A new MIMO architecture was developed to enhance the data rates in [23] to tackle the interference with simulation and detection algorithms in molecular communication. In [24], a routing protocol of UAVs in IoT, based on RPL, is introduced to support data aggregation and urgent communication, which enhances the efficiency of energy. In [25], the author proposes using UAVs in mobile edge computing networks to address remote area computational limits through an offloading strategy, and in [26], using UAVs in IoT networks for data collection and positioning. Low-altitude drones increase efficiency and accuracy, particularly in elevation. In [27], the author proposes using UAVs with delay-tolerant networking for collecting IoT data. The Hilbert Curve algorithm improves flight paths for agriculture and emergencies. In [28, 29], the author suggests merging NOMA and CR tech in 6G for UAVs, using a model and optimization. In [30], cognitive radio systems on UAVs

and intelligent surfaces improve obstructed air-to-ground communication. Successful simulations. In [31], the author discusses enhancing efficiency and privacy in a maritime cognitive UAV network using secure RSMA, CPFS algorithm, and power allocation. In [32], the author discusses using UAVs with cognitive radio for optimized surveillance, focusing on security and energy. In [33], the author explores the use of CRN technology for DSA in disaster wireless networks, addressing performance challenges. In [34], the author discusses challenges faced by Cognitive Radio-enabled UAVs for spectrum access in primary user channels and proposes solutions. In [35], a CIoT system improves IoT connections with UAVs collecting energy via RF signals and DF relaying. In [36], the author examines an EH-UAV-CRN for improved energy efficiency by adjusting transmission power and utilizing renewable energy, and in [37], using UAVs as fog nodes in IoT health monitoring for disaster and rescue operations, focusing on efficiency.

3. System Model

The examination of a Wireless Powered IoT model incorporates UAVs and IoT Devices (IoTDs), and the quantity of these vehicles is measured by M, and the quantity is measured by K. U signifies the collection of UAVs containing M elements. In contrast, C signifies the collection of IoTDs containing K elements. Each IoTD is represented as $C_k, C_k \in C = \{C_1, C_2, \ldots., C_K\}$, whereas each UAV is represented as $U_m, U_m \in U = \{U_1, U_2, \ldots, U_M\}$. The IoTDs and UAVs are deployed randomly within a square region R, where the UAVs are operated at a constant height H. Each UAV possesses a set of associated IoTDs, indicated by Ω_i, with i indicating the index value of UAVs. The total count of IoTDs is denoted as C in the system, which equates to the union of all $C = \cup_{i=1}^{M} \Omega_i$. This implies that each IoTD is linked to a single UAV based on its proximity. Those UAVs and IoTDs are equipped with specific abilities, which utilize the full-duplex model that allows them to transmit and receive information simultaneously. The UAVs deliver power to the IoTDs during downlink transmission and gather data from them during uplink transmission. Utilizing full-duplex capabilities, the IoTDs can extract the energy from the UAVs at the time of concurrent data transmission. The shared-antenna framework of each UAV consists of a singular antenna fitted with a shared-antenna duplexer, and the UAV and IoTD functions are performed in full-duplex mode. In Table 1, the important notations that are used here are illustrated. The primary goal of the system design is to increase the efficiency of the UAVs that are constructed in the full-duplex OFDMA network while adhering to the Quality of Service (QoS) restrictions of using the minimum downlink power and uplink rate. The channel is designed to include both small-scale variance and large-scale loss. The distance determines the large-scale loss, which only affects signal strength. The small-scale variation is unique for each user and is determined by frequency. The channel coefficients remain unchanged throughout each scheduling interval, which contains numerous OFDM symbols. Here, it utilizes $H_{i,j}^{n} \in \mathbb{H} = \{H_{j,k}^{UU,n}, H_{j,k}^{MM,n}, H_{j,k}^{DW,n}, H_{j,k}^{UP,n}\}$ to express the gain from i to j on subcarrier n, which indicated $H_{i,j}^{n} \neq H_{i,j}^{n}$. The overall gain across subcarrier n is mathematically expressed in Equation (1),

$$H_{i,j}^{n} = \phi_{i,j} g^{n} \tag{1}$$

In this scenario, $\phi_{i,j} = (\beta_0 d_{i,j})^{-\alpha}$ represents the product of the path loss constant β_0 and the distance between devices $i\ and\ j$, denoted by $d_{i,j}$. The path loss coefficient, denoted by α and with a minimum value of 2, determines the severity of signal attenuation. The reference distance d_0 It is set at 1 meter. The wavelength of the signal is represented by λ. Small-scale fading caused by multipath propagation is captured by g^n, which follows a Rayleigh distribution with parameters (0,1). Here, the UAVs and IoTDs have different capabilities for Successive Interference Cancellation (SIC). The power of self-interference at UAV i and its respective IoTD j on its subcarrier n is given by $\delta_{UAV} q_{i,j}^{n} p_i^{UAV,n} |G_{i,i}^{UAV,n}|^2$ and $\delta_{IoTD} q_{i,j}^{n} p_i^{IoTD,n} |G_{j,j}^{IoTD,n}|^2$ respectively. Here, δ_{UAV} and δ_{IoTD} are constant values representing the quality of SIC at UAVs and IoTDs, where $0 < \delta_{UAV} \ll 1\ and\ 0 < \delta_{IoTD} \ll 1$. The SI channel gain for UAV i is denoted by $G_{i,j}^{UAV,n} \in C$ and for IoTD j is represented by $G_{j,j}^{IoTD,n} \in C$. The subcarrier assignment indicator $q_{i,j}^{n}$ is characterized as

$$q_{i,j}^{n} = \begin{cases} 1, & if\ subcarrier\ n\ of\ UAV\ i\ is\ assigned\ to\ IoTD\ j \\ 0, & otherwise. \end{cases} \tag{2}$$

Each subcarrier on a UAV is allocated to an IoTD. Therefore, the assignment indicator must fulfil the following criteria:

$$\sum_{j=1}^{C} q_{i,j}^{n} \leq 1 \quad \forall i, i \in Uj \in C \tag{3}$$

The computed input signals are Gaussian; here, the variables $s_i^{IN,n}$ are represented as identically distributed $(i.i.d.)$ Complex Circularly Symmetric Gaussian (CSCG) random variables exhibiting a mean of zero and a variance of one. This is represented as $s_i^{IN,n} \sim CN(0,1) for\ all\ i \in C$. Without loss of generality, $s_j^{EH,n}$ as independent white sequences from any distribution with an expected value of 1 for all $i \in U$, encompassing both intra and inter-cell interference at each IoTD. Consequently, in the Downlink (DL), the energy signal is received at IoTD j on subcarrier n from UAV i and is mathematically expressed in equation (4),

$$y_{i,j}^{IoTD,n} = \sqrt{P_i^{UAV,n} H_{i,j}^{DW,n} s_i^{EH,n}} + \delta_{IoTD} \sqrt{P_j^{IoTD,n}, G_{j,j}^{IoTD,n}, s_j^{IN,n}} + \sum_{kU,k\epsilon\neq i} \sqrt{P_j^{UAV,n} H_{k,j}^{DW,n} s_k^{EH,n}} + \sum_{h\in U,h\neq i,m\in C,m\neq j} \sqrt{P_m^{IoTD,n} H_{h,m}^{MM,n} s_m^{IN,n}} + z_j^{n}, \tag{4}$$

The interaction between IoTD j and UAV i in the uplink direction is influenced by disturbance originating from other cells, self-disturbance resulting from the full-duplex mode, and ambient noise. The disturbance from other cells consists of two parts: from UAVs and IoTDs situated in different UAV cells. Consequently, the radio frequency signal that UAV i receives on subcarrier n from IoTD $j$is expressed in Equation (5):

$$y_{i,j}^{UAV,n} = \sqrt{P_i^{IoTD,n}\, H_{i,j}^{UP,n}\, s_j^{IN,n}} + \delta_{UAV}\sqrt{P_i^{UAV,n}, G_{i,i}^{UAV,n}, s_i^{EH,n}} + \sum_{kU,k\epsilon\neq i}\sqrt{P_k^{UAV,n}\, H_{k,j}^{UU,n}\, s_k^{EH,n}} + \sum_{h\in U,h\neq i,m\in C,m\neq j}\sqrt{P_m^{IoTD,n}\, H_{h,m}^{UP,n}\, s_m^{IN,n}} + z_j^n, \quad (5)$$

The SINR for UAV i when IoTD j transmits data to it on subcarrier n, and the quantity of power that IoTD j obtains from UAV i on subcarrier n, is calculated using equations (7) and (6), respectively. These equations can be found in Box I and are also shown in Equation (7). In addition, the combined transmitting power for both UAV and IoTD should not surpass their maximum capacities, respectively. $P_{UAV}^{max}\ and\ P_{IoTD}^{max}$. Let P_i^n represent the transmitting power on a subcarrier n. Thus, the limitations on power can be determined as follows:

$$\delta_{IoTD} q_{i,j}^n P_j^{IoTD,n}\left|G_{j,j}^{IoTD,n}\right|^2 + \sum_{k\epsilon U} q_{k,j}^n P_k^{UAV,n}|H_{k,j}^{DW,n}|^2 + \sum_{h\epsilon U,h\neq i,m\in C,m\neq j} q_{h,m}^n P_m^{IoTD,n}|H_{h,m}^{MM,n}|^2 \quad (6)$$

$$\sum_{n=1,\forall i,i\in U}^{N} P_i^{UAV,n} \le P_{UAV}^{max} \quad (7)$$

$$\sum_{n=1,\forall i,i\in C}^{N} P_i^{IoTD,n} \le E_{IoTD}^{max} \quad (8)$$

$$R_{UL} = \sum_{\forall j\epsilon C}\sum_{\forall i\epsilon U}\sum_{\forall N\epsilon N} R_{i,j}^{UAV,n} \quad (9)$$

$$E_{EH} = \sum_{\forall j\epsilon C}\sum_{\forall i\epsilon U}\sum_{\forall N\epsilon N} \eta_{i,j} E_{i,j}^{IoTD,n} \quad (10)$$

The overall speed at which data is transmitted from all IoTDs is referred to as R_{UL}can be computed by multiplying the total number of uplink messages by the average message size. The total harvested energy is denoted as E_{EH}, using the linear Energy Harvesting (EH) model to harvest energy from all IoT devices. This formula uses the logarithmic function. $R_{i,j}^{UAV,n} = B\log(1 + SINR_{i,j}^{UAV,n})$ to determine the harvested energy for each UAV and IoT device pair. The value of $\eta_{i,j}$, which falls between 0 and 1, represents a fixed factor that measures the harvesting effectiveness of the j^{th} IoTD at the i^{th} UAV location.

The energy consumption in a wireless-powered IoT employing M UAVs and K IoTDs, with the support of UAVs and a Full-Duplex OFDMA system, encompasses the energy expended for communication by both of them, along with the IoTDs' harvested energy. The energy consumption for each IoT $C_k \in C\ and\ UAV\ U_m \in U$, on subcarrier n, their respective transmit powers are determined by $P_k^{IoTD,n}\ and\ P_m^{UAV,n}$. The overall energy utilized for transmission is computed by adding together the transmission powers of every IoTD and UAV across all subcarriers. The energy collected from the antenna noise is typically lower than the energy harvesting device's sensitivity, so it do not consider it. The overall energy usage of the network, considering the IoTDs' energy harvesting, is computed.

$$E_{transmit} = \sum_{\forall k\in C}\sum_{n=1}^{N} P_k^{IoTD,n} + \sum_{\forall k\in U}\sum_{n=1}^{N} P_m^{UAV,n} \quad (11)$$

$$E_{total} = E_{transmit} - E_{EH} \quad (12)$$

Table 1. Symbols used to represent key variables

Notations	Description	Notations	Description
C	Grounds IoTDs count	U	UAVs count
$\boldsymbol{H_{j,k}^{UU,n}}$	Channel gain on subcarrier	$H_{j,k}^{MM,n}$	IoTD j to UAV k channel gain on subcarrier
$\boldsymbol{H_{j,k}^{DW,n}}$	Downlink Channel gain on subcarrier	$H_{j,k}^{UP,n}$	UAV j to UAV k uplink channel gain on subcarrier
$\boldsymbol{G_{i,j}^{IoTD,n}}$	IoTD on subcarrier	$G_{i,i}^{UAV,n}$	UAV i self-interference channel gain on subcarrier
$\boldsymbol{P_i^{IoTD,n}}$	IoTD i transmission power on subcarrier	$P_i^{UAV,n}$	UAV i transmission power on subcarrier
B	Subcarrier bandwidth	σ^2	Gaussian noise variance

4. Proposed Methodology

As the development of 6G Edge technology approaches, there has been a gradual emergence of various 6G technologies. One significant aspect is the use of UAVs for information sharing. These aerial vehicles function as both supplementary computing power and communication nodes in locations that are unreachable by ground vehicles or Road Side Units (RSUs). Deployments are a complicated process. Additionally, UAVs are considered as mobile nodes that provide ground units a proper view, which can be integrated with UAVs' GPS data to improve their awareness of blind spots.

Nevertheless, the restricted battery lifespan of UAVs needs to be considered to ensure safety and dependability. To tackle this problem, a probabilistic model is employed to enhance battery performance and its effect on verification outcomes for autonomous robots. Current AVs

often struggle to anticipate road hazards that are obstructed by other cars in advance, such as landslides or traffic congestion. In this regard, using UAVs to provide a bird's-eye view can offer valuable information on potential road hazards in the cooperative environment for AVs. In our execution, the significant traits of hovering UAVs are inspired by their extensive application across various sectors, such as telecommunications. Hovering capability reduces energy expenditure by minimizing unnecessary movements. Figure 1 explains the architecture of resource allocation and clustering for UAVs in a hybrid UAV network with edge-based federated learning.

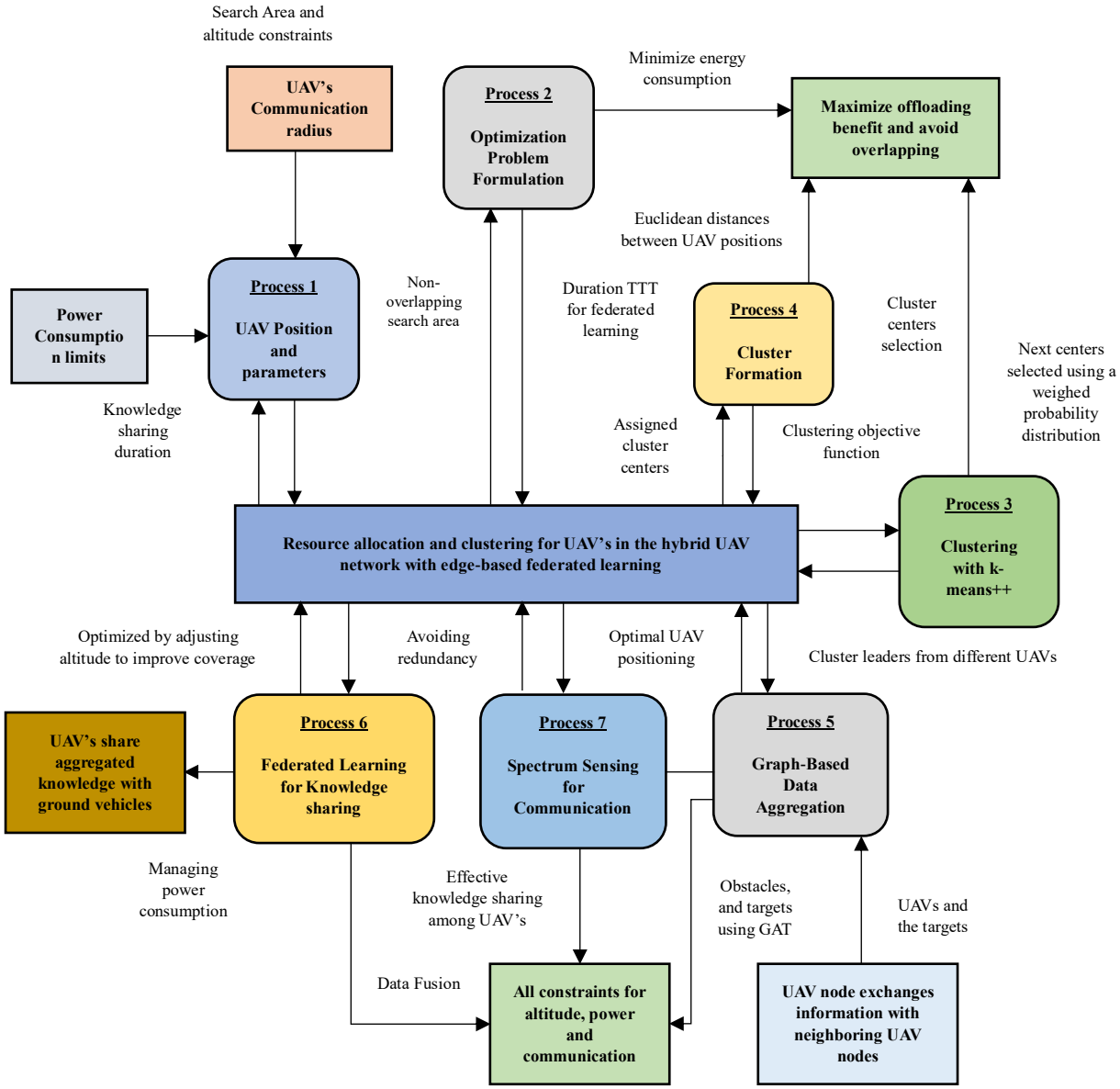

Fig. 1 Hybrid UAV network

4.1. Cluster Coverage for UAVs

A solution is proposed for the optimal allocation of resources among edges to enhance offloading for the designated UAV during data-sharing operations with ground vehicles. Offloading refers to the benefits obtained from merging insights from neighbouring UAVs. The optimization dilemma encompasses five constraints: maximum searchable altitude, non-overlapping search region, coverage restrictions, energy usage, and the collective experience enhancement. The initial constraint guarantees that UAVs function within their highest altitude threshold. The other four constraints assure that there is no overlap between UAVs, they do not surpass their altitude limits, they do not exceed their energy utilization thresholds, and they have adequate time for federated learning to data exchange. To develop the most efficient resource distribution model, a novel approach is created. By converting the optimization dilemma into a Lagrangian multiplier problem, a strong basis for discovering a solution is required. Through continuous refinement and an emphasis on accuracy and effectiveness, it becomes essential to attain optimal resource allocation. Figure 2 explains the UAV resource allocation optimization process in detail.

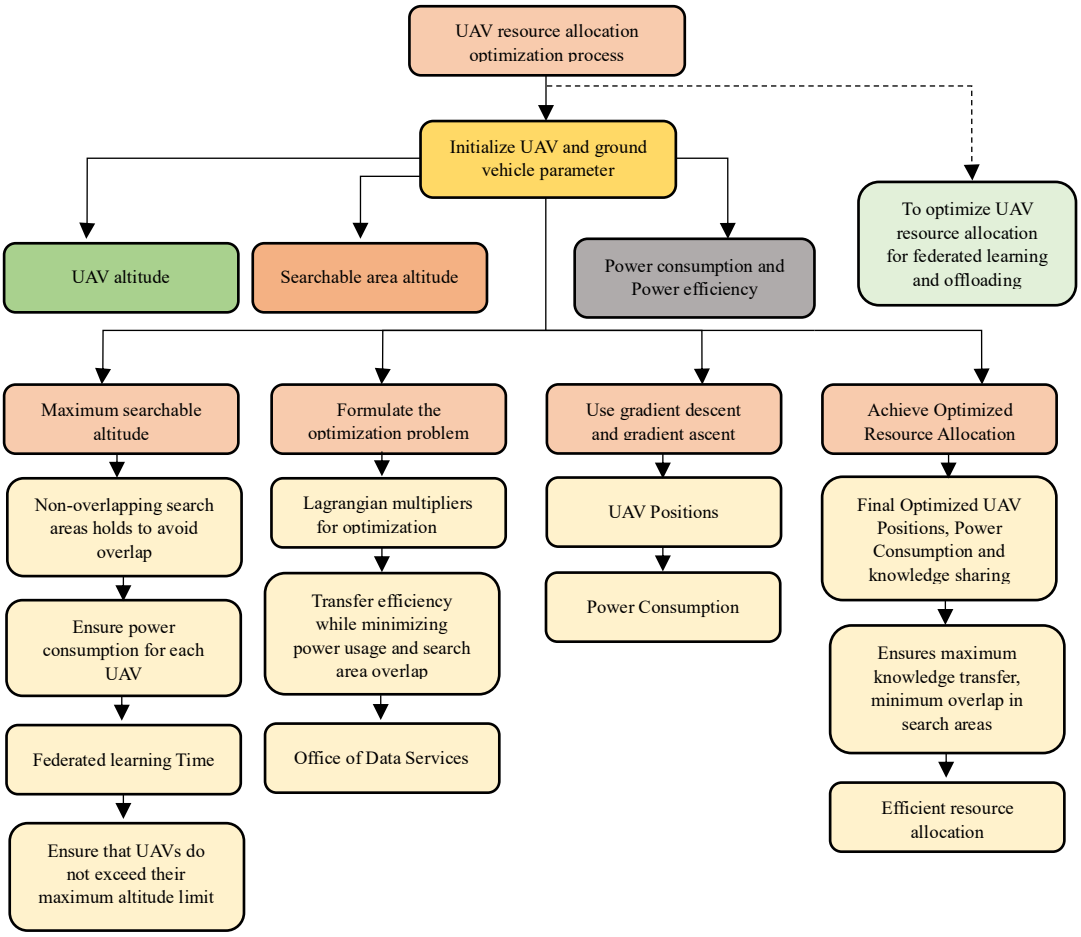

Fig. 2 UAV resource allocation optimization process

4.1.1. Objective Function

To optimize the offloading efficiency, consider power limitations and reduce redundancy.

$$Maximize\ \sum_{i=1}^{n} A_i - \sum_{i=1}^{n} \lambda_i (h_i - z_i) - \sum_{i \neq j}^{n} \mu_{ij} \left((x_i - x_j)^2 + (y_i - y_j)^2 - (r_i + r_j)^2 \right) - \sum_{i=1}^{n} \beta_i (z_i - Z_{max}) - \sum_{i,j}^{n} \gamma_{ij} (d_{ij} - v_j T) + \xi \sum_{i \neq j}^{n} \eta_{ij} - \sum_{i=1}^{n} \delta_i (P_i - P_{maxi}) - \sum_{i=1}^{n} \varepsilon_i (P_i - \eta_i (C_i + D_i)) \quad (13)$$

4.1.2. Constraints

The minimum searchable height constraint is the smallest allowed height for a searchable item.

$$h_i - z_i \geq 0 \quad (14)$$

The altitude from the ground surface is referred to as z_i. The Non-overlapping Search Areas Constraint. To guarantee that the search zones of UAVs do not intersect, for every i *and* j where i is equal to j.

$$(x_i - x_j)^2 + (y_i - y_j)^2 \geq (r_i + r_j)^2$$
$$z_i \leq Z_{max} \quad (15)$$

$$\frac{d_{ij}}{v_j} \leq T \quad (16)$$

$$P_i \leq Z_{max,i} \quad (17)$$

$$P_i = \eta_i (C_i + D_i) \quad (18)$$

Boundary restriction, Z_{max} refers to the highest altitude threshold that the UAVs can reach—a limitation on the transfer of knowledge. T implies the federated learning-based time requirements, which are evident that the ground vehicle is able to transfer the UAV information within a designated timeframe. *R*estrictions on power consumption ensure that the UAV i does not utilize more energy than its allocated upper limit. A model for estimating power usage describes how the amount of energy used is connected to the level of computing required and the distance travelled, factoring in. η_i As a measure of power efficiency, the ground vehicles follow a consistent constraint when receiving data from each UAV, performing this in order and within the conical beam of every UAV. The Lagrange multipliers for each constraint, including ξ, which balances the compromise between enhancing knowledge transfer and reducing redundancy, are represented by $\lambda_i, \mu_{ij}, \beta_i, \gamma_{ij}, \eta_{ij}, \delta_i$ *and* ε_i. This composition seeks to meet the objectives of enhancing knowledge transfer and preventing overlap while also guaranteeing uniform data reception by terrestrial vehicles. It furthermore integrates federated learning and employs the parallel processing concept to enable effective knowledge aggregation, and it is described in Algorithm 1.

Algorithm.1 The procedure for enhancing the performance of UAVs

Input: Number of uncrewed aerial vehicles n, Duration for collaborative learning T, Upper boundary for maximum height Z_{max}, Balance factor ξ

Output: Optimized values for the UAV's parameters, Lagrange multipliers, and the maximum objective value.

Start by setting up the parameters for both the UAV and the Ground Vehicle.
For each UA $i\ in\ 1\ to\ n$ do
    Initialize $h_i, r_i, x_i, y_i, P_{max,i}, \eta_i, C_i, D_i, A_i$
For each ground vehicle j do
    Initialize v_j
Begin by setting up Lagrange multipliers.
Initialize $\lambda_i, \mu_{ij}, \beta_i, \gamma_{ij}, \delta_i, \epsilon_i$
Procedure constraints: Max searchable height: $h_i - z_i \geq 0$ non-overlapping areas: $\left(x_i - x_j\right)^2 + \left(y_i - y_j\right)^2 \geq \left(r_i + r_j\right)^2$ boundary: $z_i \leq Z_{max}$ knowledge transfer: $\frac{d_{ij}}{v_j} \leq T$ power consumption: $P_i \leq P_{max,i}$ power model: $P_i = \eta_i(C_i + D_i)$
Procedure objective function: $objective \leftarrow \sum_{i=1}^{n} A_i - \xi \sum_{i,j} \gamma_{ij}\left(d_{ij} - v_j T\right)$ return $objective$
Procedure Lagrangian: $L \leftarrow OBJECTIVE\ FUNCTION\ for\ each\ UAV\ i\ do\ L-= \lambda_i(h_i - z_i) + \delta_i\left(P_i - P_{max,i}\right) + \varepsilon_i(P_i - \eta_i(C_i + D_i))$
For each UAV pair $i, j\ where\ i \neq j\ do$
    $L-= \mu_{ij}\left(\left(x_i - x_j\right)^2 + \left(y_i - y_j\right)^2 - \left(r_i + r_j\right)^2\right) + \gamma_{ij}(d_{ij} - v_j^T)$
For each UAV i do
    $L-= \beta_i(z_i - Z_{max})$
Return L
Method Optimize: Set up the parameters for both the uncrewed aerial vehicle and the terrain vehicle, and set up the Lagrange multipliers.
While $iteration <$ max$_iterations$ do
    $iteration \leftarrow iteration + 1\ L_{current} \leftarrow LAGRANGIAN for\ each\ UAV\ i\ do$
        Update h_i, r_i, x_i, y_i, P_i using gradient descent
    For each constraint, do
        Update $\lambda_i, \mu_{ij}, \beta_i, \gamma_{ij}, \delta_i, \epsilon_i$ using gradient ascent
    If $abs(L_{current} - LAGRANGIAN) < TOLERANCE$ then
        break
    retrieve characteristics of uncrewed aerial vehicles, coefficients used in Lagrangian optimization, and the primary function to be optimized.
Call Main

4.2. Cluster Formation for UAVs

Clustering is an important method used in unsupervised learning models to categorize objects based on their shared and distinctive traits within each dataset. Its primary objective is to cluster similar data while ensuring that data in separate clusters remain notably different. While k-means is a popularly applied clustering algorithm, it strongly depends on the initial choice of cluster centers, which can significantly influence the outcomes. To address this issue, k-means++ was developed, which selects the first seeds with the notation that they should be far apart from each other. In this approach, the first center is picked randomly, with the following centers being picked by a weighted approach based on a probability distribution. This has been a better method, which has performed better in practice application than other enhanced k-means algorithms. Although other alternatives exist, k-means++ still remains a popular choice due to its efficient calculation and the ability to achieve the best results. The goal of this optimization function can be mathematically expressed as follows:

$$EM = \sum_{i=1}^{k} \sum_{U \in Ci} ||P_U - P_i||_2^2 \quad (19)$$

The total of the squared Euclidean distances from each UAV location to its corresponding center of cluster is referred to as EM. The number of clusters is represented by k, while P_U signifies the UAV position. P_i refers to the center of a cluster C_i. The step-by-step process of the k-means++ model is given in Algorithm 2.

Algorithm 2 K-means++

Data: Location information of N UAVs, Parameter k
Result: k clusters

Choose the first cluster center randomly from the UAV locations;
For each iteration from $2\ to\ k$:

Calculate the distance of each data point from the previous cluster center.
For $j = 1\ to\ N$ data points:
Find the shortest distance D(Ui) between each UAV and the cluster center;
Generate a random number for selection.
Select a new cluster center based on the probability proportional to $D(U_i)$;
End iteration.
For $k = 1\ to$ maximum number of iterations:
Assign each UAV to its nearest cluster center.
Recalculate the cluster center.
If there is no change in the result:
Stop iteration.
Output the final clustering results.

All UAVs within a cluster are of equal importance, but the initial one is assigned the role of the Cluster Head (CH). The other in the group interacts with the CH in a periodic way to obtain details regarding their environment. Leaders from different clusters engage in two-way communication to share a broader understanding of the situation, promoting agreement. Ultimately, the head of each cluster relays its situational awareness to the other UAVs.

4.3. Intelligent Graph-based Learning Model (IGLM)

In this section, a Collaborative Searching Model (CSM) is developed using IGLM to create the graph model. The group of adjacent cooperative nodes, like (N_k^a, N_k^o and N_k^t) with surrounding agent k can be represented as:

$$N_k^a = \{l \in V_a : ||p_k - p_l|| \le d_k, k \ne l\} \quad (20)$$

$$N_k^o = \{c \in V_o : ||p_k - p_c|| \le d_k\} \quad (21)$$

$$N_k^t = \{m \in V_t : ||p_k - p_m|| \le d_k\} \quad (22)$$

From equations (20), (21), and (22), the terms $p_k, p_l, p_m\ and\ p_c$ are the centers of obstacles, where $p_k = [x_k, y_k]^T, p_l = [x_l, y_l]^T,\ p_m = [x_m, y_m]^T\ and\ p_c = [x_c, y_c]^T, d_k$ denoted the circular region of radius, V_a denotes the node set of agents. After establishing communication, agents proceed to exchange information. The agent's detection range determines the obstacle set of the agent's neighbors. The set of obstacles is denoted by V_o. Similarly, the target set of neighboring agents for agent k is determined by the agent's detection range. The GAT plays a critical role in gathering graph-based data, with V_t representing the node set of targets and $V_a \cup V_o \cup V_t = V$. In the CSM setting, IGLM was created especially to compile an agent's observation data, which includes three key components: Query, Key, and Value. The agent's current position serves as the Query, while the positions of neighboring agents, targets, and obstacles act as the Key (K^a, K^o, K^t). The high-dimensional features of the observation information $h_k = \sigma(\xi^k W_k)$ are denoted as the Value, with $\sigma(.)$ being the Relu function and W_k representing the network weight. The attention weight in GNN can be defined as

$$e_a^{(k,l)}(Query, K^a) = \begin{cases} \exp(-b_a ||p_k - p_l||, l \epsilon N_k^a \\ 0, \quad otherwise \end{cases} \quad (23)$$

$$e_o^{(k,c)}(Query, K^o) = \begin{cases} \exp(-b_o ||p_k - p_c||, c \epsilon N_k^o \\ 0, \quad otherwise \end{cases} \quad (24)$$

$$e_a^{(k,m)}(Query, K^t) = \begin{cases} \exp(-b_t ||p_k - p_m||, l \epsilon N_k^t \\ 0, \quad otherwise \end{cases} \quad (25)$$

The attention weights for neighbouring agents, obstacles, and targets of agent k are denoted as $e_a^{(k,l)}$, $e_a^{(k,c)}$, and $e_a^{(k,m)}$. b_a, b_o, and b_t represent the corresponding coefficients. To ensure proper scaling, the attention weights are normalized using a softmax function. Hence, the combination characteristics of various kinds of nodes may be stated as follows.

$$\alpha_a^{(k,l)} = \begin{cases} softmax\left(e_a^{(k,l)}\right) = \frac{\exp(e_a^{(k,l)})}{\sum_{l \epsilon N_k^a} \exp(e_a^{(k,l)})}, \exists l \epsilon N_k^a \\ o, \quad otherwise \end{cases} \quad (26)$$

$$\alpha_o^{(k,c)} = \begin{cases} softmax\left(e_o^{(k,c)}\right) = \frac{\exp(e_o^{(k,c)})}{\sum_{l \epsilon N_k^o} \exp(e_o^{(k,c)})}, \exists l \epsilon N_k^o \\ o, \quad otherwise \end{cases} \quad (27)$$

$$\alpha_a^{(k,l)} = \begin{cases} softmax\left(e_a^{(k,l)}\right) = \frac{\exp(e_a^{(k,l)})}{\sum_{l \epsilon N_k^a} \exp(e_a^{(k,l)})}, \exists l \epsilon N_k^a \\ o, \quad otherwise \end{cases} \quad (28)$$

$$h_k^a = \sum_{l \epsilon N_k^a} \alpha_a^{(k,l)} h_a^{(k,l)} \quad (29)$$

$$h_k^o = \sum_{c \epsilon N_k^o} \alpha_o^{(k,c)} h_o^{(k,c)} \quad (30)$$

$$h_k^t = \sum_{m \epsilon N_k^t} \alpha_t^{(k,m)} h_t^{(k,m)} \quad (31)$$

The high-dimensional features of neighboring agents, obstacles, and targets for agent k are denoted as $h_a^{(k,l)}$, $h_o^{(k,c)}$, and $h_t^{(k,m)}$. To maintain consistency in dimensions, the features are aggregated and then dimensionally transformed. The output features of IGLM are obtained through a sequence of interconnected operations. The operation of catenation is denoted by $(.||.)$, while W_k^a, W_k^o, and W_k^t represent the weights of networks that are not

influenced by the size of the obstacles and agents. Therefore, IGLM can adjust the policy network to various settings with varying quantities of agents and obstacles.

$$h'_k = \sigma(h_k^a W_k^a || h_k^o W_k^o || h_k^t W_k^t) \quad (32)$$

4.4. UAVs throughput Analysis

As a result of incorporating spectrum sensing into the transmission process, two key factors contribute to the success of data packet delivery: (1) UAVs receiving the Left-Hand Side (LHS) signals through forward links; and (2) accurate detection of spectrum usage by Primary User (PU) signals through detectors on UAVs.

4.4.1. Packet Dropout

To evaluate the likelihood of packet loss in UAV communications, the typical method used is to implement the Gilbert-Elliott (GE) model utilizing a two-state discrete Markov model. The GE model studies the relationships between packet dropout, which may result from receiver malfunctions and channel conditions (particularly in UAV situations where multipath effects prevail). In this research, the Markov-based GE model is introduced due to its capability to integrate Ricean fading, which is mainly utilized to understand the time-varying characteristics of packet dropout. The model features two states: good ($identified\ as\ "g"$) and bad ($identified\ as\ "b"$). The Markov process is depicted in Figure 3, which is defined by its probabilities such as $p_{gg}, p_{gb}, p_{bb}\ and\ p_{bg}$. In this context, p_{xy} indicates the likelihood of transitioning from state x to state y. The stationary distributions for both the positive and negative states are represented as $\pi_g\ and\ \pi_b$, correspondingly. This can be expressed using the following equations:

$$p_{gg} = 1 - p_{gb}, p_{bb} = 1 - p_{bg}; \pi_g = \frac{p_{bg}}{p_{gb}+p_{bg}}, \pi_b = \frac{p_{gb}}{p_{gb}+p_{bg}} \quad (33)$$

The Ricean distribution is used to represent the Ricean fading model, and it utilizes two parameters to describe the amplitude of the received signal. The symbol κ represents the ratio of the direct signal's influence compared to the scattered signal's influence. Ω represents the power of the incoming signal, which is influenced by both range and path loss via the direct link. The signal power detected at the reference distance of d_0 is denoted as Ω_0. In UAV applications, the path loss exponent η is usually established as 2 to align with the free space model. With a specified receiver sensitivity S_r, the probability of a timely error can be articulated as:

$$v^2 = \frac{\kappa\Omega}{1+\kappa}, \omega^2 = \frac{\Omega}{2(1+\kappa)} \quad (34)$$

$$\Omega = \Omega_0 (\frac{d}{d_0})^{-\eta} \quad (35)$$

$$p_g(t) = 1 - Q\left(\frac{v}{\omega}, \frac{\sqrt{2Sr}}{\omega}\right) \quad (36)$$

Q. represents the Marcum Q-function. The indicated packet dropout rate. P_d is therefore referred to as the estimated value. The value of φ_0 is equal to 1. The sum of N_p multiplied by $p_g(t)$ Each observation is represented as $\varphi_0 = \frac{1}{N_p}\sum_t p_g(t)$. The total number of observations is denoted as N_p. As a result, the anticipated opportunity number for each upload is indicated by:

$$E[N_d] = (f_c(n_e) - 1)(1 - P_d)n_0 + (1 - P_d) f_c(f_{rem}(\lambda_F T_0, n_o)) \quad (37)$$

The worth of n_e, representing the count of E-MAVLink frames for a single LHS, is calculated using the equation $n_e = \frac{F}{n_0} = \frac{\lambda_F T_0}{n_o}$. The function f_c elevates the element to the closest greater value. The function calculates the remainder after division.

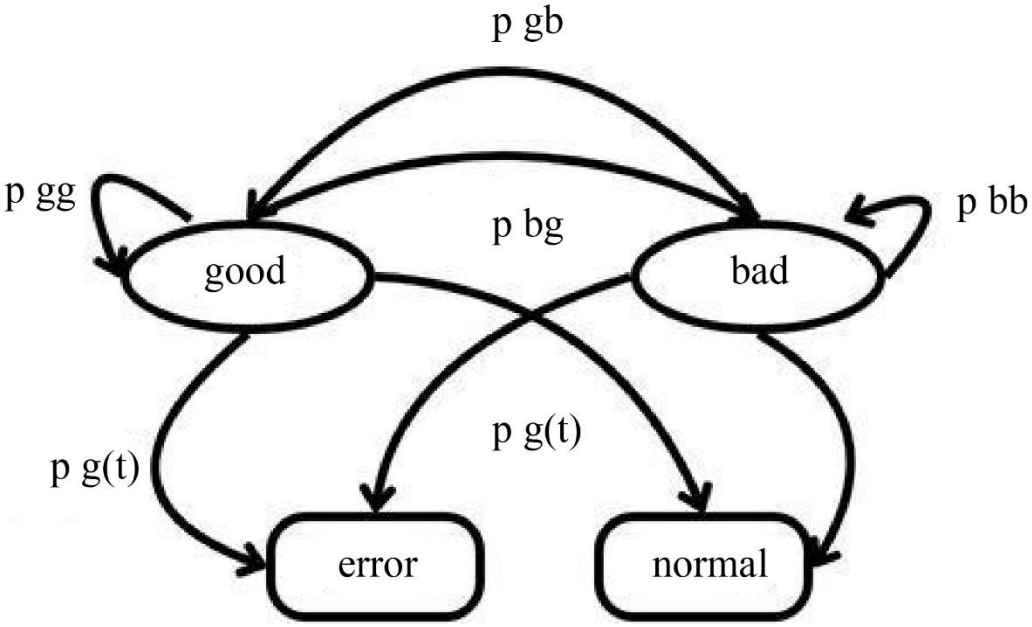

Fig. 3 The state transition diagram is built upon a two-state markov process

4.4.2. Spectrum Sensing

This section explores a unified method for detecting spectrum availability, considering the existence of a spectrum sensing system before transmission and various kinds of connections. This method, known as energy detection, combines the energy from samples within a specific bandwidth and compares it to a predetermined threshold. Since there might be various sub-channels to analyse the integration of multiple narrow-band spectrum detectors, which is denoted as $D(m,n)$, where m denotes the link index from the total M and n signifies the index values of N channels. Consequently, identifying PU signals in the narrow-band channels across various links is denoted as $s(m,n,t)$. A binary hypothesis testing framework is subsequently established to reflect the ON/OFF condition of PU signals.

$$y(m,n,t) = \begin{cases} n_i(m,n,t) & : H_0 \\ h(m,n,t)s(m,n,t) + n_i(m,n,t) & : H_1 \end{cases} \quad (38)$$

The observed samples $y(m,n,t)$ on the mth link are received by a detector $D(m,n)$. The sample of Primary User (PUs) signals is represented by $s(m,n,t)$. The channel gain of the detector and the PUs are denoted by $h(m,n,t)$, while $n_i(m,n,t)$ represents the noise conferring to the AWGN model. The variable t represents the chosen sensing time, and the value. H_0 indicates the absence of any signal, whereas H_1 signifies the presence of PUs signals. AWGN models and a zero-mean Circular Symmetric Complex Gaussian (CSCG) random vector are grounded, as well as the probability of detection P_D For one, the narrow bandwidth is mathematically expressed in Equation (39).

$$P_D(m,n) = P_r(y(m,n,t) > \lambda_D(m,n); H_1) = Q\left(\frac{\lambda_D(m,n) - N(\sigma_s(m,n)^2 + \sigma_n(m,n)^2)}{\sqrt{2N(\sigma_s(m,n)^2 + \sigma_n(m,n)^2)^2}}\right) \quad (39)$$

The signal variance among individual channels is represented by σ_s, while the threshold for determining whether the state is ON or OFF is denoted by λ_D. The probability of a false alarm, P_F, is defined as:

$$P_F(m,n) = \Pr(y(m,n,t) > \lambda_D(m,n); H_0) = Q(\sqrt{N}\frac{\lambda_D(m,n) - \sigma_n(m,n)^2}{\sigma_n(m,n)^2}) \quad (40)$$

Due to greater emphasis on avoiding false alarms rather than ensuring high detection rates, the decision guideline is created that employs a Constant Detection Rate (CDR) standard. It presumes a central chi-square distribution Q and approximates y as a normal distribution. The threshold value is represented as λ_D for the narrow channel n over m link based on a specific detection probability P_D.

In this formula, σ_n signifies the noise's standard deviation, Q is a function that adheres to a normal distribution with the expression $Q(x) = 1/\sqrt{2\pi}\int_x^\infty e^{-s2/2}ds$, from x to infinity, and $N = F_s.T_{sen}$ shows the length of the sample used for estimation at the time of T_{sen} period.

When several n detectors are permitted to determine link possession across m links. This is a kind of fusion policy that concurs with a decision-making process when the individual detector ranges. N_k. The following equations provide the fused detection probability. P_D and false alarm probability P_F for many detectors working on the connections m.

$$\lambda_D(m,n) = \sigma_n(m,n)^2 Q^{-1}(P_D(m,n))\sqrt{\frac{2\sigma_s(m,n)^2 + \sigma_n(m,n)^2}{N\sigma_n(m,n)^2}} + \sigma_s(m,n)^2 + \sigma_n(m,n)^2 \quad (41)$$

$$P_{un}(m) = \sum_{i=Nk}^{Nn} C(i,N_n)\prod_{j=1}^{i} p_{un}(m,j)\prod_{j=i+1}^{Nn}(1 - P_{un}(m,j)) \quad (42)$$

The detection probability is represented by $un = 'D'$, while $un = 'F'$ stands for the probability of a false alarm. One important aspect to consider is that the detection probability $P\hat{}D(m)$ in the CDR criteria is determined based on the design requirements. As a result, the likelihood of false alarm $P\hat{}F(m)$ is a significant factor that impacts the performance of the detector.

4.4.3. Saturation throughput

The standard approach for assessing the effectiveness of an end-to-end MAC model is to measure saturation throughput. In this evaluation, it is expected that users transmit C2 messages at a rate of 1 per second. The saturation throughput mainly incorporates three elements: uplink packet loss, opportunity loss stemming from non-optimal spectrum detector delays, and missed detections occurring during the sensing phase. Here, the term C_3 is utilized to signify scenarios where the UAV inaccurately identifies a link. The re-sensing mechanism is used to adhere to a binomial distribution. When the Max-N-RS scheme is implemented, the Probability Mass Function (PMF) of the C3 scenario for $T_i(k)$ link opportunities across R re-sensing periods can be expressed as:

$$Pra(T_iC_3 = r,k)) = \binom{R}{r} PF(T_i(k))^r (1 - PF(T_i(k)))^{R-r} \quad (43)$$

From Equation (43), the index r signifies access behaviors. Assuming a limit of R attempts for re-sensing, the probability of failing to identify a link of k^{th} UAV is represented as $Pra(T_i(c3 = R,k) = PF(T_i(k))^R$. To facilitate the calculation of throughput, the transmission rate and detection probability remain constant across the links and detectors. If a delay occurs in the sensing phase, there exists a chance for a chosen spectrum opportunity, which gets eliminated by E-MAC, which can be illustrated as:

$$Pr_I[N(t > T_D)] = ReLu(\frac{\lambda_F T_0 K - (n_t - e^{TD\lambda v})}{\lambda_F T_0 K}) \quad (44)$$

The variable n_t represents a value, named T_0M, which is calculated as 1 over the sum of the reciprocals of $\lambda_v \; and \; \lambda_a$. The time delay, denoted as T_D, is modeled by adding the values $\delta_T + T_{sen}PF\mathrm{R}$. The function ReLu has the structure of $ReLu(x) = max(0, x)$. The theory of order statistics for measuring probability is concentrated. The exponential distribution of random variables is expressed in the expected value of the first n variables as $E\left[X_{(n)}\right] = 1/\lambda(1 + \frac{1}{2} + \frac{1}{3} + \cdots . + \frac{1}{n}) \approx \frac{logn}{\beta}$. Therefore, $n_t - \exp(T_D\lambda_v)$ represents the maximum number of opportunities with longer durations than TD. With a total number of received opportunities $\lambda_F T_0 K$, it may apply a ReLu function to guarantee a positive probability and denote $E[L]$ as the mean Duration for the link without accounting for time delays, and $E[L_a]$ for link duration with time delays. Hence, following its traversal through the E-MAC layer and the value of $E[L_a]$ is represented below:

$$\frac{E[L_a]}{E[L]} = \frac{\int_{TD}^{+\infty} x\lambda_v e^{-\lambda v x} dx}{\int_0^{+\infty} x\lambda_v e^{-\lambda v x} dx} \tag{45}$$

$$E[L_a] = E[L](\lambda_v T_D + 1)$$

The saturation throughput model for a UAV is developed using Equations (37, 42, 44, 45). This model takes into account elements such as latency, imperfect on-board detection, and loss of packets. The value of $\bar{G}$, representing the theoretical throughput with stationary connections, can be determined by using the MLE method to calculate λ_F Moreover, another obstacle is estimating $E[L]$. There exist two situations to evaluate based on the connection between the count of $UAVs\ (K)$ and the count of links (M). If K is greater than M, this is considered a spectrum-scarce environment where all links must be allocated using an allocation algorithm. In this situation, the designated opportunity duration adheres to an exponential distribution with $E[L] = 1/\lambda v$; however, when K is less than M, which is referred to as a spectrum-dense setting, solely the K opportunities are utilized in each allocation cycle. By employing statistical theory and the order statistics framework, it can be ascertained that the mean opportunity duration in this context is represented as $E[L] = \sum(1/j)K\lambda v$ where j varies from $M - K + 1 \; to \; M$. Consequently, it reformulates the throughput model for each UAV as a piecewise function. Through simulations, it has been observed that there is a transition between two equations about the use of resources.

Additionally, the iterative procedure might not consistently assign the top K resources, especially when K equals M. To address this issue, an empirical equation has been introduced that considers a more precise relationship between spectrum resources and the number of users. This refined model for throughput is represented as:

$$Th_{UAV} = \frac{GE[N_d]\left(1-PrI\left(N(t\geq T_D)\right)\right)(1-Pra(C_3=R))(E[L_a]-T_D)}{T_0} = G(fc(ne)-1)(1-Pd)n_0 + (1-Pd)fc\left(f_{rem}(\lambda_F T_0, no)\right)\left(1 - ReLu\left(\frac{\lambda_F T_0 K - (n_t - e^{TD\lambda v})}{\lambda_F T_0 K}\right)\right).\left(\frac{1-Pf\left(T_i(k)\right)^R E[L](\lambda_v(\delta_T + T_{sen}P_F R)+1)}{T_0}\right) \tag{46}$$

$$Th_{UAV} = \begin{cases} \frac{Th}{\lambda_v} & : M \leq K \\ Th.\left(\frac{\sum_{n=M-K+1}^{M}\sum_{j=M-n+1}^{M}\left(\frac{1}{j}\right)}{K\lambda_0}(\lambda_v T_D + 1) - T_D\right) & : M > K \end{cases} \tag{47}$$

$$Th_{UAV} = \begin{cases} \frac{Th}{\lambda_v} & : M \leq K \\ Th.\left(\frac{\sum_{n=M-K+1}^{M}\sum_{j=M-n+1}^{M}\left(\frac{1}{j}\right)}{K\lambda_v}\left(\lambda_{ca}^{\frac{\lambda pM}{Kca}}(\lambda_v T_D + 1) + 1\right) - T_D\right) & : M > K \end{cases} \tag{48}$$

$$T_D = \begin{cases} \delta_T + T_{sen} & P_F\left(T_i(k)\right)R \leq 1 \\ \delta_T + T_{sen}\,, P_F\left(T_i(k)\right)R \leq 1 & 1 < P_F\left(T_i(k)\right)R \leq R \end{cases} \tag{49}$$

$$\frac{\lambda_F T_0}{n_0} = \begin{cases} 1 & \frac{\lambda_F T_0}{n_0} < 1 \\ \frac{\lambda_F T_0}{n_0} & \frac{\lambda_F T_0}{n_0} \geq 1 \end{cases} \tag{50}$$

The coefficients $C_a \; and \; \lambda_{ca}$ are utilized to modify the spectrum resources. When $(\frac{\lambda_v M}{KC_a})$ is significant, indicating a lack of resources, the throughput is anticipated to resemble that of $M <= K$ with a reduced opportunity duration. On the other hand, in a spectrum-rich setting, the opportunity duration extends. Because the E-MAC layer-based re-sensing number is invariably greater than one, a function is necessary to gauge its impact on the E-MAC.

5. Performance Analysis

The analysis encompasses 120 tasks with the number of UAVs varying from 5 to 40. The experiment was repeated 100 times for each scenario, and the outcomes were then averaged. The results are compared with the earlier methods like Clustering-based Consensus-based Bundle Algorithm (CCBBA) [1], Distributed Edge-based Collaborative Knowledge Sharing (DECKS) [3], and Multi-Objective Optimization Problem in UAV (MOOPU) [5]. Table 2 and Figure 4 compare CCBBA, DECKS, MOOPU, and the proposed ILHCHU method. Figure 4 illustrates that as the quantity of UAVs rises, the communication steps correspondingly rise for all four approaches. CCBBA and DECKS have exponential growth step-wise with communication, whereas MOOPU has a linear progression. Conversely, the proposed ILHCHU model exhibits a significantly slower increment in communication procedures, which ensures a smooth communication load despite having bigger UAV fleets.

The communication overhead in ILHCHU is less as it has an effective clustering policy that minimizes unnecessary communication requirements. As the number of UAVs grows, DECKS and CCBBA require two-way communication within the system. ILHCHU effectively limits this through the means of controlled communication in clusters. The result is a more scalable and efficient

solution in the case of increasing the number of UAVs. The tables and Figures 2 and 4 depict that under a limited count of UAVs, all the other algorithms, CCBBA, DECKS, MOOPU, and the proposed ILHCHU demonstrate more unassigned tasks and reduced completion rate. In this stage, the UAV system is not able to deal with the workload; thus, there is an even distribution of the task completion rate with all other algorithms. Table 2 and Figure 4 show that the task scores produced in the four approaches, CCBBA, DECKS, MOOPU, and the proposed ILHCHU, are somewhat similar. The increased advantage of ILHCHU does not affect the overall score and the rates of task completion. The processing time of the four algorithms increases with an increase in the quantity of UAVs, as shown in Table 3 and Figure 5. The running times of ILHCHU and CCBBA are similar, as the former is slightly higher than the latter. Compared to ILHCHU and CCBBA, DECKS is slower to execute, although it takes more communication steps in CCBBA. The longevity of operation is quite impressive when compared with the four methodologies of MOOPU. Therefore, ILHCHU effectively optimizes the interaction of communication between different tasks and sizes of UAVs and does not significantly affect the overall performance and the rate of full achievement of tasks.

Table 2. Performance analysis of communication steps, unassigned tasks, and total score

UAVs	No. of. Communication Steps				No. of. Unassigned tasks				No. of. Total Score			
	CCBBA	DECKS	MOOPU	ILHCHU	CCBBA	DECKS	MOOPU	ILHCHU	CCBBA	DECKS	MOOPU	ILHCHU
5	10000	20000	30000	5000	100	100	100	100	3000	4000	5000	2000
10	20000	40000	50000	10000	90	90	90	90	5000	6000	7000	4000
15	25000	60000	70000	15000	70	70	70	80	6000	7000	8000	5000
20	35000	90000	10000	20000	60	60	60	60	8000	9000	10000	7000
25	40000	12000	15000	25000	50	50	50	50	9000	10000	11000	8000
30	50000	15000	20000	50000	40	40	40	40	11000	12000	13000	10000
35	70000	17000	25000	65000	30	30	30	30	12000	13000	14000	11000
40	80000	20000	30000	70000	20	20	20	20	13000	14000	15000	12000

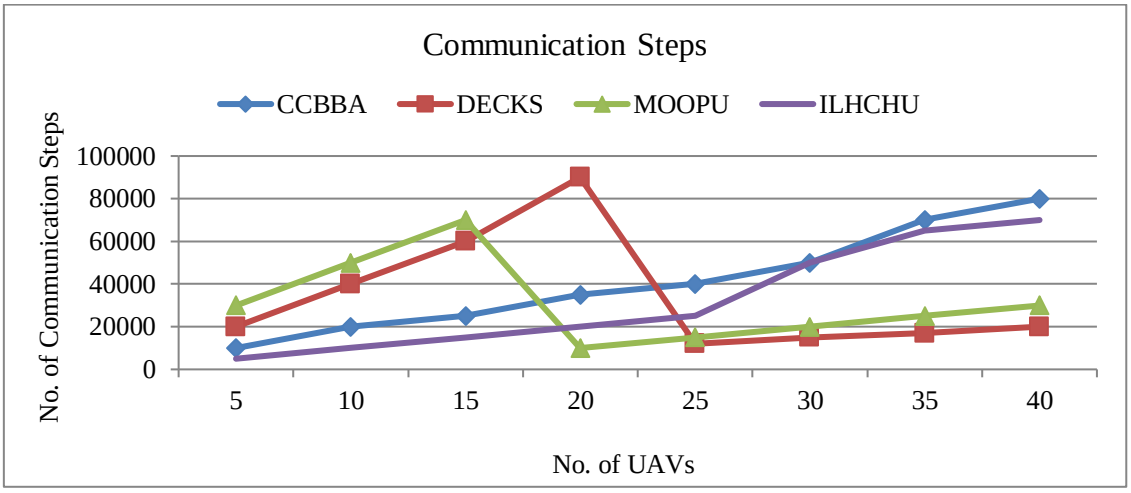

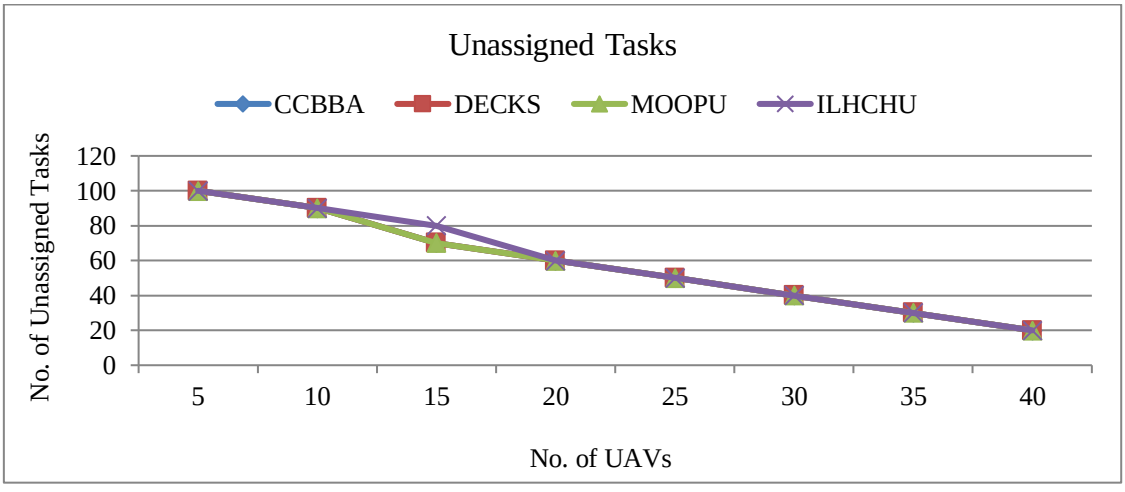

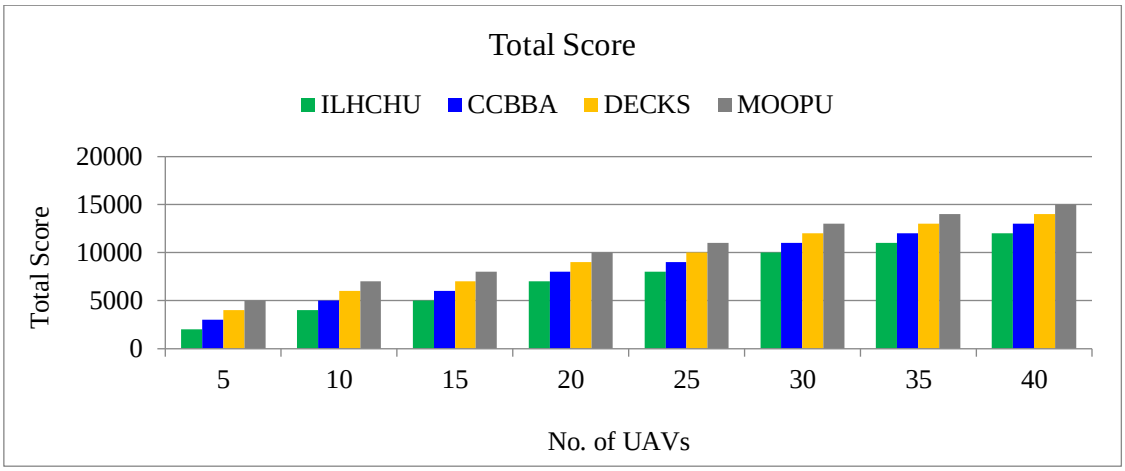

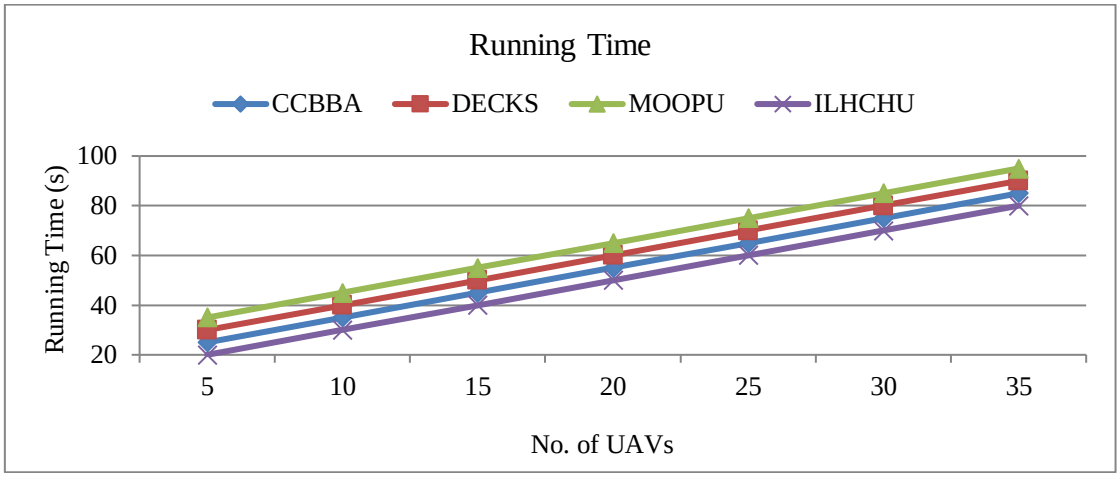

Fig. 4 No of UAVs vs. Communication steps, no of UAVs vs. Unassigned tasks, no of UAVs vs. Total scores, and no of UAVs vs. Running times

Table 3. Performance analysis of running time, time consumed, and energy consumption

UAVs	No. of. Running Time				No. of. Time Consumed				UAVs	Energy Consumption			
	CCBBA	DECKS	MOOPU	ILHCHU	CCBBA	DECKS	MOOPU	ILHCHU		CCBBA	DECKS	MOOPU	ILHCHU
5	25	30	35	20	600	300	400	250	**10**	100	120	130	150
10	35	40	45	30	450	200	350	220	**20**	200	210	230	270
15	45	50	55	40	500	180	370	210	**30**	300	320	330	380
20	55	60	65	50	520	160	400	200	**40**	400	430	430	490
25	65	70	75	60	540	150	420	195	**50**	500	530	550	610
30	75	80	85	70	550	140	430	190	**60**	600	640	660	750
35	85	90	95	80	560	140	440	185					

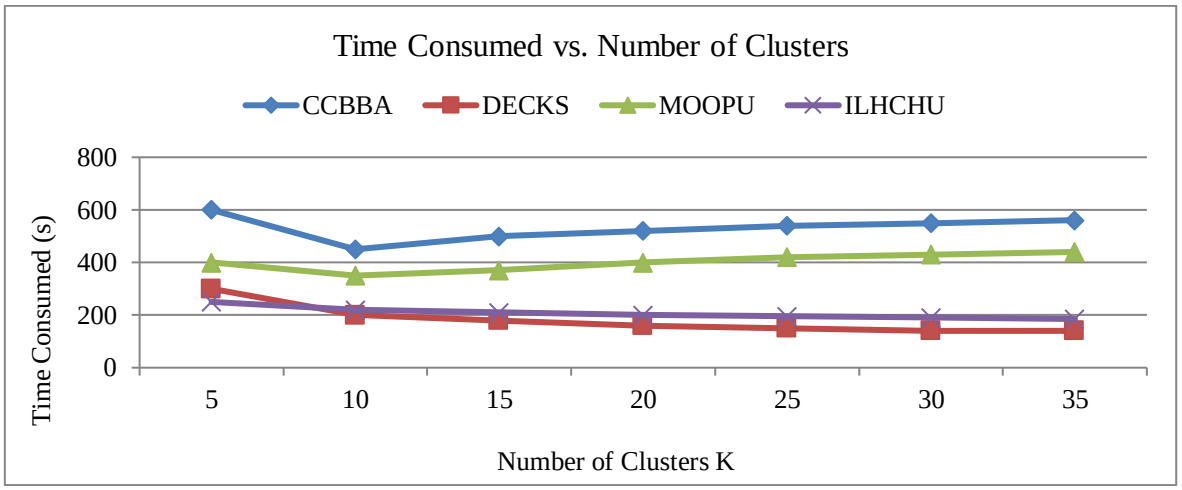

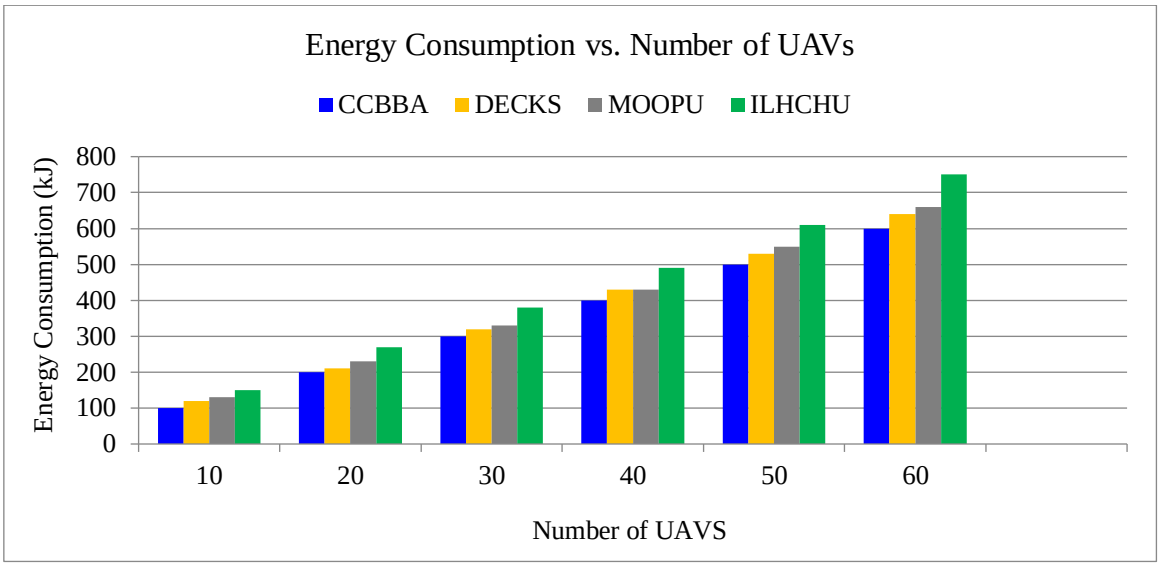

Fig. 5 No of Clusters vs. Time consumed (s), and no of UAVs vs. Energy consumption (kJ)

Table 3 and Figure 5 represent the time of four algorithms - CCBBA, DECKS, MOOPU, and the Proposed ILHCHU - regarding the number of UAVs. The results indicate that DECKS has always had the lowest values of time spent, and its value remains relatively constant despite the increase in the quantity of UAVs due to its efficient task distribution strategy. Since the time usage of the UAVs in ILHCHU is consistent and controlled, the time use grows steadily and constantly with the increase in the UAV count in comparison to CCBBA and MOOPU. ILHCHU achieves it by organizing the communication load and task distribution effectively. The CCBBA and MOOPU time usage is more variable and high-consuming, particularly when the UAVs are more than 20 units. The time consumption of MOOPU is also increasing steadily, which points to the complexity of the computations as the UAVs increases. Also, CCBBA, which is better than MOOPU, requires much more time than ILHCHU due to its ineffective communication and task allocation strategies. Overall, ILHCHU is very well-balanced in terms of efficiency and flexibility, which makes it highly suitable for large UAV networks.

Figure 5 illustrates the effect of the UAV count on the proposed method, ILHCHU, in a predetermined target area, of 500 meters by 500 meters in size. This paper presents the comparison between the coverage rates and repeated coverage rates of the six algorithms, CCBBA, DECKS, MOOPU, and ILHCHU, of varying UAV numbers, 10, 20, 30, 40, 50, and 60 UAVs. Table 4 and Figure 5 illustrate the coverage rates associated with changes in the number of UAVs, and each bar represents the repetitive coverage rate. As the UAV count increases, the coverage rate of all six algorithms increases; however, at varying rates. However, some of the algorithms, like CCBBA and DECKS, are likely to undergo premature convergence, which often results in a coverage rate that is lower than the optimal coverage of 90. Moreover, the coverage by CCBBA is always greater in comparison to that of DECKS due to poor coordination of UAVs. DECKS slightly beats CCBBA and demonstrates slight increases in repeated coverages, which indicates the difficulties of optimization of UAV location. MOOPU and ILHCHU show a significant improvement in performance. The achievement of the full coverage rate of 100% in the case of 40 UAVs and the progressive decline in the coverage rates (as low as 21% - 22.4%) is all due to its ingenious adaptive height control option, which makes ILHCHU the best of all models. This will reduce the overlapping of the UAVs and reduce the interference in communication, which will lead to a viable utilization of the resources. Table 4 and Figure 6 indicate that the consumption patterns of energy are as follows. The data reveals that the amount of energy used by ILHCHU is a little bit higher than that used by DECKS and MOOPU, but with the highest coverage of areas and minimum redundancy. There is a higher energy use in CCBBA and DECKS due to poor energy optimization strategies, and Moopu shows a better proportionality between coverage and energy productivity, though not to the overall performance of ILHCHU. ILHCHU demonstrates great flexibility in the deployment of multiple UAVs to achieve optimal coverage, minimum redundancy, and affordable energy usage. This feature makes it especially suitable for those cases that involve different numbers of UAVs.

An examination is carried out on the way the communication stages of the algorithm are influenced by different cluster amounts through 100 Monte Carlo simulations, while ensuring that the starting conditions stay the same. The scenario includes 10 uniform UAVs and 20 assignments, with the quantity of clusters varying from 1 to 10. Table 4 and Figure 6 display the mean communication stages across 100 simulations. As the quantity of clusters increases from 9, it is identified that a reduction in the number of communication stages is necessary for addressing internal conflicts. This reduction is due to having fewer UAVs in each cluster. This decrease leads to a lesser volume of information being relayed to the lead UAV within the cluster. Figure 6 highlights a

simultaneous growth in the communication steps required for resolving external conflicts, as UAV leaders from various clusters need to share more information. This trend in inter-cluster communication is realized in CCBBA and DECKS, which results in significant overhead. When the number of clusters is above 10 (k=10), the necessity to use internal conflict resolution is limited, and all UAVs begin to interact in a bidirectional manner, such as the CBBA approach. MOOPU is partially dealing with this issue through the use of hierarchical clustering, but it remains inefficient due to increased demands on addressing external conflicts. The proposed ILHCHU demonstrates outstanding results in the performance of the well-balanced approach to conflict resolution. It facilitates internal communication through the facilitation of effective coordination inside a cluster and reduces external communication in a well-organized information exchange plan between different clusters. Unlike the existing CCBBA, DECKS, and MOOPU systems, ILHCHU not only minimizes the overhead in the two-way communication but also ensures no conflict in assigning tasks. The best thing about ILHCHU is that it minimises the total number of communication steps, particularly when the cluster count is large. This improvement makes ILHCHU more scalable and efficient, especially when it comes to situations where large-scale operations of UAVs are to be allocated.

Table 4. Performance analysis of coverage rate, repeated coverage rate, and number. of. communication steps and communication composition

UAVs	Coverage Rate and Repeated Coverage Rate								No. of. Com. Steps		Communication Composition			
	CCBBA	DECKS	MOOPU	ILHCHU	CCBBA	DECKS	MOOPU	ILHCHU	No. Cl	CCBBA	Int. Com.	Ext. Com	Int. Com.	Ext. Com
10	20	15	25	27	5	4	6	8	**2**	1000	350	50	10	5
									3	1500	340	70	12	7
20	50	45	55	58	10	9	12	14	**4**	2000	330	100	8	6
									5	2500	320	150	11	8
30	70	68	72	74	15	14	17	19	**6**	3000	310	200	10	7
									7	3500	300	300	9	8
40	85	80	88	89	20	18	22	24	**8**	4000	290	400	10	7
50	90	88	93	93	25	23	26	28	**9**	4500	280	500	12	6
60	95	93	97	97	30	27	31	33	**10**	5000	270	600	11	8

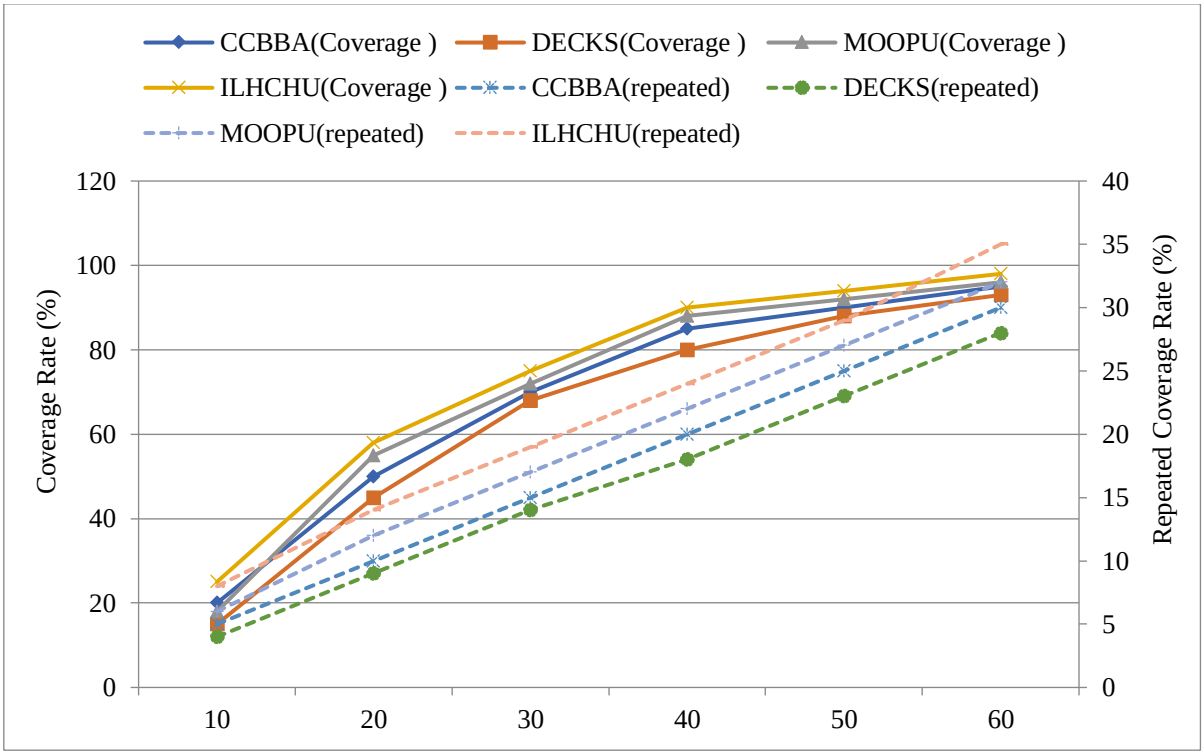

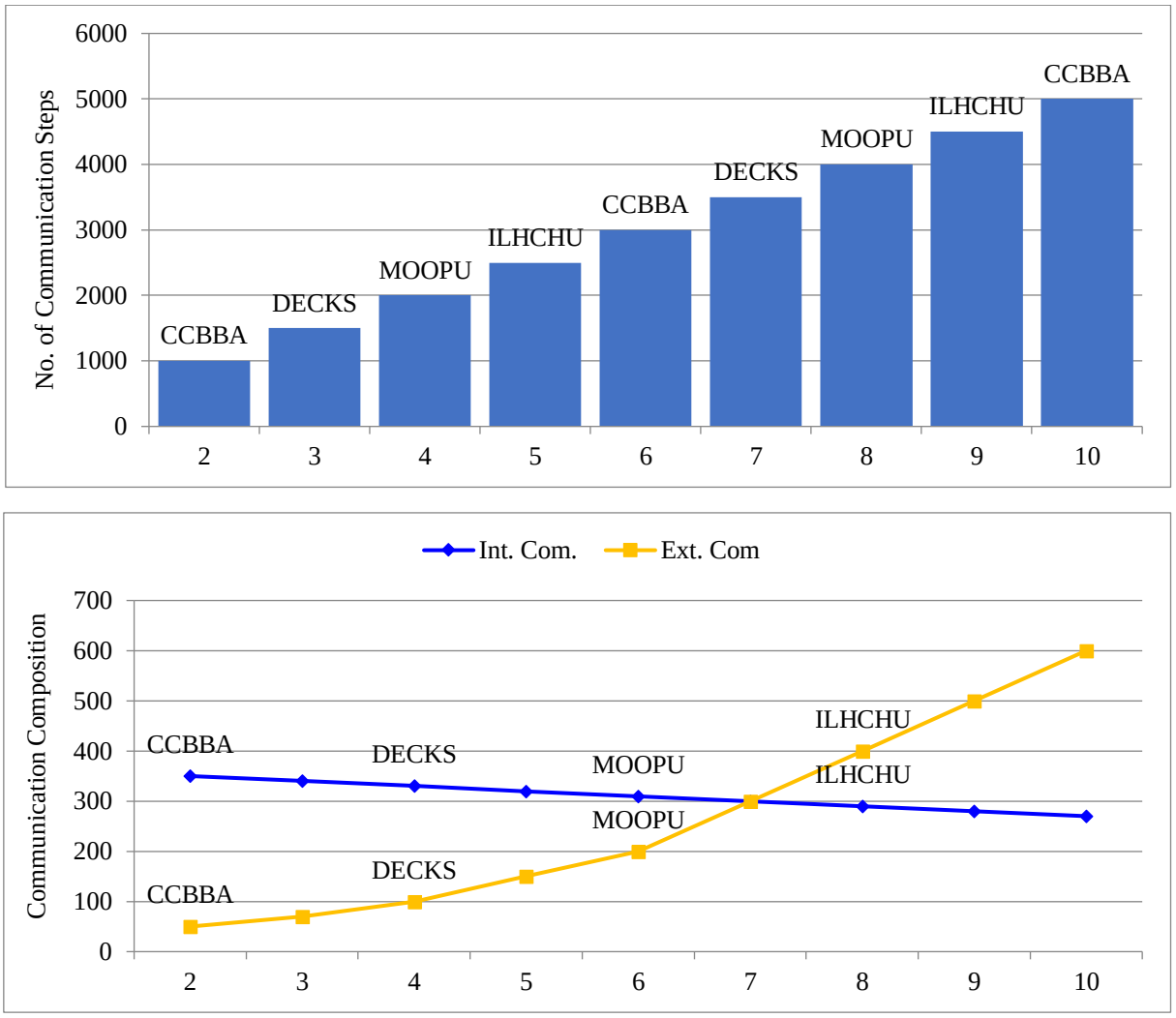

Fig. 6 No of UAVs vs. Coverage rate (%), no of Clusters vs. Communication steps, and no of Clusters vs. Communication composition

6. Conclusion

Enhancing the performance of communication and energy consumption in UAV-IoT networks, in the case of uplink communication and full-duplex mode. The algorithms of optimization addressed the main problem of interference, power limitations, and energy harvesting. The signal quality measurement was also improved with more accurate calculation of SINR, taking into account environmental noise, self-interference, and inter-cell interference, improved resource allocation in case of power constraint by using Lagrangian multiplier algorithm to balance the power-performance and energy-efficiency. A linear-driven EH model was proposed to be used with IoTDs and UAVs, with logarithmic operation for measuring the energy harvested in order to achieve maximum efficiency. The integration of UAVs into 6G edge networks has demonstrated how it can provide reliable communication at difficult-to-reach sites and enhance situational awareness in tasks of hazard detection and environmental monitoring. Other strategies that were implemented to optimize resources included altitude limitations, eliminating overlap in search zones, and proper management of power consumption. This led to effective scheduling and the exchange of knowledge in various groups. The UAV communication has been optimized by using clustering techniques like k-means++ that optimize the formation of clusters and coordination among the clusters. IGLM was capable of integrating both spatial and situational data with high levels of flexibility in a constantly shifting environment. The Gillett-Elliott model was used to measure the percentage of packet loss in order to take into account fundamental differences of the channel, thereby improving the reliability of the communication linkage between the UAV and the base station. The implementation of federated learning has increased the level of collaboration in decision-making because data privacy has been preserved. The framework demonstrated tremendous energy efficiency, reliability of communication, and optimization of resources in hybrid UAV-IoT Networks. Based on this measure the ILHCHU model is compared with CCBBA, DECKS and MOOPU, these existing methods and attained the minimum number of the communication steps at 70000, 20 unassigned tasks, a lower total score of 12000, a running time of 80, time consumed of 185, higher energy consumption score of 750, and coverage rate and repeated coverage rate of 97 and 33 respectively and communication steps of 5000 and a communication composition of 8 was all achieved by The

innovations are easy to modify and tailor to the upcoming generation of technology such as 6G, which opens the possibilities of innovative and green UAV-IoT systems. Future studies might explore the investigation of dynamic mobility patterns, real-time analytics, and optimizations that will be performed with the help of AI in order to address more complex cases and enhance the stability of the system.

References

[1] Maisam Ali et al., "Decision-Based Routing for Unmanned Aerial Vehicles and Internet of Things Networks," *Applied Sciences*, vol. 13, no. 4, pp. 1-17, 2023. [CrossRef] [Google Scholar] [Publisher Link]

[2] Brindha Subburaj et al., "A Self-Adaptive Trajectory Optimization Algorithm Using Fuzzy Logic for Mobile Edge Computing System Assisted by Unmanned Aerial Vehicle," *Drones*, vol. 7, no. 4, pp. 1-19, 2023. [CrossRef] [Google Scholar] [Publisher Link]

[3] Hongxia Zhang et al., "Resource Allocation and Offloading Strategy for UAV-Assisted LEO Satellite Edge Computing," *Drones*, vol. 7, no. 6, pp. 1-20, 2023. [CrossRef] [Google Scholar] [Publisher Link]

[4] S. Agnes Shifani, "Revolutionary Solutions for Vehicular Networks: Pollution Monitoring and Cluster-based Resource Management," *2025 International Conference on Electronics and Renewable Systems (ICEARS)*, Tuticorin, India, pp. 807-812, 2025. [CrossRef] [Google Scholar] [Publisher Link]

[5] Jinyi Zhao et al., "Multi-Objective Optimization for EE-SE Tradeoff in Space-Air-Ground Internet of Things Networks," *Electronics*, vol. 12, no. 12, pp. 1-20, 2023. [CrossRef] [Google Scholar] [Publisher Link]

[6] M. Tamilselvi, "Innovative Wireless Communication Solutions: IoT Mobility in Smart Cities, and 5G-V2X Resource Management," *2025 International Conference on Electronics and Renewable Systems (ICEARS)*, Tuticorin, India, pp. 719-724, 2025. [CrossRef] [Google Scholar] [Publisher Link]

[7] Shuqi Wang et al., "Trajectory Planning for UAV-Assisted Data Collection in IoT Network: A Double Deep Q Network Approach," *Electronics*, vol. 13, no. 8, pp. 1-16, 2024. [CrossRef] [Google Scholar] [Publisher Link]

[8] Xuan-Toan Dang, and Oh-Soon Shin, "Optimization of Energy Efficiency for Federated Learning over Unmanned Aerial Vehicle Communication Networks," *Electronics*, vol. 13, no. 10, pp. 1-23, 2024. [CrossRef] [Google Scholar] [Publisher Link]

[9] J. Josiah Samuel Raj, and Anitha Gopalan, "Compact Bi-slot Patch Antenna with Tapered Edges for Ka-Band Applications Featuring Machine Learning-Assisted Performance Prediction," *International Journal of Environment, Engineering and Education*, vol. 7, no. 3, pp. 196-207, 2025. [CrossRef] [Google Scholar] [Publisher Link]

[10] Guoku Jia, Chengming Li, and Mengtang Li, "Energy-Efficient Trajectory Planning for Smart Sensing in IoT Networks Using Quadrotor UAVs," *Sensors*, vol. 22, no. 22, pp. 1-20, 2022. [CrossRef] [Google Scholar] [Publisher Link]

[11] Sang Quang Nguyen et al., "Exploiting User Clustering and Fixed Power Allocation for Multi-Antenna UAV-Assisted IoT Systems," *Sensors*, vol. 23, no. 12, pp. 1-32, 2023. [CrossRef] [Google Scholar] [Publisher Link]

[12] Syed Luqman Shah et al., "An Innovative Clustering Hierarchical Protocol for Data Collection from Remote Wireless Sensor Networks Based Internet of Things Applications," *Sensors*, vol. 23, no. 12, pp. 1-26, 2023. [CrossRef] [Google Scholar] [Publisher Link]

[13] Lihan Liu et al., "Delay-Informed Intelligent Formation Control for UAV-Assisted IoT Application," *Sensors*, vol. 23, no. 13, pp. 1-21, 2023. [CrossRef] [Google Scholar] [Publisher Link]

[14] Mohamed Ould-Elhassen Aoueileyine et al., "Coverage Strategy for Small-Cell UAV-Based Networks in IoT Environment," *Sensors*, vol. 23, no. 21, pp. 1-21, 2023. [CrossRef] [Google Scholar] [Publisher Link]

[15] Wei Zhuang, Fanan Xing, and Yuhang Lu "Task Offloading Strategy for Unmanned Aerial Vehicle Power Inspection Based on Deep Reinforcement Learning," *Sensors*, vol. 24, no. 7, pp. 1-19, 2024. [CrossRef] [Google Scholar] [Publisher Link]

[16] Mohamed Abdel-Basset et al., "Evolution-based Energy-Efficient Data Collection System for UAV-supported IoT: Differential Evolution with Population Size Optimization Mechanism," *Expert Systems with Applications*, vol. 245, pp. 1-20, 2024. [CrossRef] [Google Scholar] [Publisher Link]

[17] Zhixiong Chen, Jiawei Yang, and Zhenyu Zhou, "UAV-Assisted MEC Offloading Strategy with Peak AOI Boundary Optimization: A Method based on DDQN," *Digital Communications and Networks*, vol. 10, no. 6, pp. 1790-1803, 2024. [CrossRef] [Google Scholar] [Publisher Link]

[18] Prakhar Consul, Ishan Budhiraja, and Deepak Garg, "Deep Reinforcement Learning Based Reliable Data Transmission Scheme for Internet of Underwater Things in 5G and Beyond Networks," *Procedia Computer Science*, vol. 235, pp. 1752-1760, 2024. [CrossRef] [Google Scholar] [Publisher Link]

[19] Xue-Yong Yu et al., "UAV-Assisted Cooperative Offloading Energy Efficiency System for Mobile Edge Computing," *Digital Communications and Networks*, vol. 10, no. 1, pp. 16-24, 2024. [CrossRef] [Google Scholar] [Publisher Link]

[20] Chuan'an Wang et al, "A UAV Migration-based Decision-Making Scheme for on-demand Service in 6G Network," *Alexandria Engineering Journal*, vol. 69, pp. 25-33, 2023. [CrossRef] [Google Scholar] [Publisher Link]

[21] Xiaobin Xu et al., "A Blockchain-Enabled Energy-Efficient Data Collection System for UAV-Assisted IoT," *IEEE Internet of Things Journal*, vol. 8, no. 4, pp. 2431-2443, 2021. [CrossRef] [Google Scholar] [Publisher Link]

[22] Alia Asheralieva, and Dusit Niyato et al., "Distributed Dynamic Resource Management and Pricing in the IoT Systems with Blockchain-as-a-Service and UAV-Enabled Mobile Edge Computing," *IEEE Internet of Things Journal*, vol. 7, no. 3, pp. 1974-1993, 2020. [CrossRef] [Google Scholar] [Publisher Link]

[23] Bon-Hong Koo et al, "Molecular MIMO: From Theory to Prototype," *IEEE Journal on Selected Areas in Communications*, vol. 34, no. 3, pp. 600-614, 2016. [CrossRef] [Google Scholar] [Publisher Link]
[24] Zhutian Yang et al., "UEE-RPL: A UAV-Based Energy Efficient Routing for Internet of Things," *IEEE Transactions on Green Communications and Networking*, vol. 5, no. 3, pp. 1333-1344, 2021. [CrossRef] [Google Scholar] [Publisher Link]
[25] Yi Liu, Shengli Xie, and Yan Zhang, "Cooperative Offloading and Resource Management for UAV-Enabled Mobile Edge Computing in Power IoT System," *IEEE Transactions on Vehicular Technology*, vol. 69, no. 10, pp. 12229-12239, 2020. [CrossRef] [Google Scholar] [Publisher Link]
[26] Zijie Wang, and Rongke Liu, "Energy-Efficient Data Collection and Device Positioning in UAV-Assisted IoT," *IEEE Internet of Things Journal*, vol. 7, no. 2, pp. 1122-1139, 2020. [CrossRef] [Google Scholar] [Publisher Link]
[27] Hengshuo Liang et al., "Internet of Things Data Collection Using Unmanned Aerial Vehicles in Infrastructure Free Environments," *IEEE Access*, vol. 8, pp. 3932-3944, 2020. [CrossRef] [Google Scholar] [Publisher Link]
[28] Yongjun Xu et al., "Robust Resource Allocation Algorithm for Energy-Harvesting-Based D2D Communication Underlaying UAV-Assisted Networks," *IEEE Internet of Things Journal*, vol. 8, no. 23, pp. 17161-17171, 2021. [CrossRef] [Google Scholar] [Publisher Link]
[29] Senhao Zhao et al., "Optimization of Effective Throughput in NOMA-Based Cognitive UAV Short-Packet Communication," *Applied Sciences*, vol. 13, no. 1, pp. 1-15, 2023. [CrossRef] [Google Scholar] [Publisher Link]
[30] Liang Zhou et al., "RIS-Enabled UAV Cognitive Radio Networks: Trajectory Design and Resource Allocation," *Information*, vol. 14, no. 2, pp. 1-15, 2023. [CrossRef] [Google Scholar] [Publisher Link]
[31] Lingtong Min et al., "Secure Rate-Splitting Multiple Access for Maritime Cognitive Radio Network: Power Allocation and UAV's Location Optimization," *Journal of Marine Science and Engineering*, vol. 11, no. 5, pp. 1-14, 2023. [CrossRef] [Google Scholar] [Publisher Link]
[32] Waqas Khalid, Heejung Yu, and Song Noh, "Residual Energy Analysis in Cognitive Radios with Energy Harvesting UAV under Reliability and Secrecy Constraints," *Sensors*, vol. 20, no. 10, pp. 1-19, 2020. [CrossRef] [Google Scholar] [Publisher Link]
[33] Amr Amrallah et al, "Enhanced Dynamic Spectrum Access in UAV Wireless Networks for Post-Disaster Area Surveillance System: A Multi-Player Multi-Armed Bandit Approach," *Sensors*, vol. 21, no. 23, pp. 1-19, 2021. [CrossRef] [Google Scholar] [Publisher Link]
[34] Weiheng Jiang et al., "Multi-Agent Reinforcement Learning for Joint Cooperative Spectrum Sensing and Channel Access in Cognitive UAV Networks," *Sensors*, vol. 22, no. 4, pp. 1-20, 2022. [CrossRef] [Google Scholar] [Publisher Link]
[35] Muhammad Rashid Ramzan et al., "Radio Resource Management in Energy Harvesting Cooperative Cognitive UAV Assisted IoT Networks: A Multi-objective Approach," *Digital Communications and Networks*, vol. 10, no. 4, pp. 1088-1102, 2024. [CrossRef] [Google Scholar] [Publisher Link]
[36] He Xiao et al., "Energy Efficient Resource Allocation in Delay-aware UAV-based Cognitive Radio Networks with Energy Harvesting," *Sustainable Energy Technologies and Assessments*, vol. 45, 2021. [CrossRef] [Google Scholar] [Publisher Link]
[37] Abdenacer Naouri et al., "Maximizing UAV Fog Deployment Efficiency for Critical Rescue Operations: A Multi-Objective Optimization Approach," *Future Generation Computer Systems*, vol. 159, pp. 255-271, 2024. [CrossRef] [Google Scholar] [Publisher Link]